ISSN 0023-1584, Kinetics and Catalysis, 2007, Vol. 48, No. 6, pp. 803–811. © MAIK "Nauka/Interperiodica" (Russia), 2007.
Original Russian Text © O.V. Komova, A.V. Simakov, G.A. Kovalenko, N.A. Rudina, T.V. Chuenko, N.A. Kulikovskaya, 2007, published in Kinetika i Kataliz, 2007, Vol. 48, No. 6, pp. 860–869.

Formation of a Nickel Catalyst on the Surface of Aluminosilicate Supports for the Synthesis of Catalytic Fibrous Carbon

O. V. Komova, A. V. Simakov, G. A. Kovalenko, N. A. Rudina, T. V. Chuenko, and N. A. Kulikovskaya

Boreskov Institute of Catalysis, Siberian Branch, Russian Academy of Sciences, Novosibirsk, 630090 Russia
e-mail: komova@catalysis.ru

Received March 14, 2006; in final form, December 26, 2006

Abstract—Conditions for the homogeneous precipitation of nickel hydroxide in the presence of urea onto the surface of aluminosilicate honeycomb monoliths, which were prepared based on clay, talc, and amorphous aluminum hydroxide, were examined. Factors affecting the concentration of supported nickel (synthesis time, starting solution concentrations, loaded amount of the support, and support calcination temperature) were studied. The possibility of supporting nickel hydroxide onto the surface of cellular ceramic foam, glass foam, and haydite was demonstrated. The morphology of nickel hydroxide particles, nickel metal particles on support surfaces, and carbon coatings synthesized in the course of the catalytic pyrolysis of a propane–butane mixture was studied by scanning electron microscopy.

DOI: 10.1134/S0023158407060079

INTRODUCTION

Catalytic fibrous carbon (CFC) prepared by the catalytic pyrolysis of various hydrocarbons exhibits unique physicochemical characteristics. This allows one to use efficiently CFC as adsorbents, supports, and catalysts for various processes [1–11]. Supports based on CFC are mainly obtained as granules. However, in the last few years, considerable attention has been focused on the synthesis of a fibrous carbon layer on the surfaces of various macrostructured inorganic supports made as honeycomb monoliths, steel gauze, fiberglass, glass cloth, and special metal filters [12–19]. This allows one to combine the unique properties of CFC with the geometric shape and mechanical strength of an inorganic matrix, which exhibits low hydrodynamic and gas-dynamic resistance.

In order to synthesize CFC, a catalyst for the pyrolysis of hydrocarbons is initially formed on the surface of a support. In the majority of publications, supported nickel metal (Ni^0) was used as this catalyst. The particle size of nickel metal and the uniformity and homogeneity of nickel distribution on the support surface are responsible for the properties and morphology of the synthesized carbon layer [20–23].

The impregnation of a support with an aqueous or aqueous alcoholic solution of a nickel salt followed by the reduction of supported nickel compounds with hydrogen is the most commonly used method for the formation of a nickel catalyst for pyrolysis [12, 13, 20, 21]. The use of an organic solvent in the impregnating solution is necessary when the inorganic matrix exhibits pronounced hydrophobic properties. In this case, the support surface is fully wetted with the nickel salt solution and the dispersity of supported nickel increases [22, 24]. Thus, for example, Keller et al. [12] managed to synthesize a mechanically strong dense CFC layer as a result of the impregnation of glass cloth with an aqueous ethanol solution of nickel nitrate. On the other hand, Ismagilov et al. [13] reported the formation of a nickel catalyst of nonuniform particle size and the synthesis of CFC weakly bound to the surface upon supporting nickel onto the surface of glass cloth by impregnation with an aqueous solution of nickel nitrate. Tribolet and Kiwi-Minsker [14] synthesized a structurally heterogeneous CFC layer on the surface of metal filters using an aqueous solution of $Ni(NO_3)_2$.

Homogeneous precipitation is another method for supporting metal (including nickel) hydroxides onto the surface of inorganic supports [25–29]. This method is based on the slow decomposition of urea in aqueous solutions of nickel salts at 85 ± 5°C:

$$CO(NH_2)_2 + 3H_2O \longrightarrow 2OH^- + 2NH_4^+ + CO_2. \quad (1)$$

The resulting OH^- ions react with Ni^{2+} to form colloidal hydroxide particles. The homogeneous precipitation method allows one to obtain more uniform and homogeneous transition metal (Ni, Co, Y, etc.) hydroxide coatings on the surfaces of inorganic supports, as compared with those prepared by the impregnation method. It is well known that the precipitate synthesized under these conditions has the structure of α-$Ni(OH)_2$ with intercalated NO_3^- and CO_3^{2-} ions [28–30].

The rate of homogeneous precipitation of nickel hydroxide depends on the rate of decomposition of urea [28, 31]. In this case, the presence of a support in the

reaction medium does not change the reaction kinetics of nickel hydroxide precipitation [28]. It was found that, unlike the samples prepared by the impregnation method, a redistribution of nickel over the support surface did not occur in the course of the subsequent drying [25, 26]. An additional advantage of this method is that any nonporous inorganic matrices, including macrostructured supports, can be used as supports [28]. However, in spite of the obvious advantages of the homogeneous precipitation method, publications concerning the use of this method in the preparation of catalysts for hydrocarbon pyrolysis are very scarce [28, 32].

The aim of this work was to study the conditions of formation of a nickel catalyst on the surfaces of ceramic aluminosilicate supports with various microstructures (honeycomb monoliths, cellular ceramic foam, glass foam, and haydite) by the homogeneous precipitation of nickel hydroxide in the presence of urea, to examine parameters affecting the concentration of supported nickel hydroxide particles, and to synthesize CFC on the supported nickel catalysts in the course of pyrolysis of a propane–butane mixture.

EXPERIMENTAL

Ceramic aluminosilicate supports with various geometric shapes (honeycomb monoliths, cellular foam materials, and granules) were used as starting matrices for the supporting of a nickel catalyst and the synthesis of a CFC layer.

The honeycomb monoliths (M) were prepared using a mixture of natural minerals (clay, talc, and amorphous aluminum hydroxide), which were taken in a stoichiometric ratio corresponding to the cordierite phase $2MgO \cdot 2Al_2O_3 \cdot 5SiO_2$ [33, 34] and subjected to mechanical treatment in a VTsM-25 vibrating centrifugal mill. Honeycomb monoliths with circular and hexagonal cross sections were prepared using extrusion molding. The honeycomb monoliths with a circular cross section had the following geometric dimensions: external diameter of a monolith, 20 mm; length, 20–50 mm; square-section channel size, 2×2 mm; number of channels per square centimeter, ~17; channel wall thickness, 0.5 mm. The honeycomb monoliths with a hexagonal cross section had a hexagon side length of 20 mm, a block length of 10–70 mm, triangle-section channels with a side of 2 mm, a wall thickness of 0.4 mm, and a number of channels per square centimeter of ~40. The resulting monoliths were calcined at 900, 1030, 1100, and 1200°C. In this case, the shrinkage of blocks was 4, 7, 9, and 14%, respectively. In accordance with the calcination temperature, the honeycomb monoliths were designated as M/900, M/1030, M/1100, and M/1200, respectively. The calculated geometric specific surface areas of M/900, M/1030, M/1100, and M/1200 were similar and equal to 21.6, 23.1, 21.0, and 19.9 cm^2/g, respectively.

The X-ray diffraction analysis performed previously [34] demonstrated that talc was the main crystalline phase of the support at a calcination temperature of 900°C. The other phases—$2MgO \cdot 2Al_2O_3 \cdot 5SiO_2$ (cordierite), α-SiO_2 (quartz), $3Al_2O_3 \cdot 2SiO_2$ (mullite), and $MgO \cdot SiO_2$ (enstatite)—were detected in small amounts. Upon calcination at 1200°C, the main crystalline phase was cordierite. Quartz, mullite, and enstatite phases were detected only in trace amounts.

The cellular ceramic foam (Powder Metallurgy Research Institute, Minsk, Belarus) had an openwork macrostructure as a three-dimensional network with an average cell size of ~2 mm. The density of the ceramics was ~0.6 g/cm^3, and the free-volume fraction was ~70%. This ceramic foam support was calcined at 1400°C. The X-ray diffraction analysis performed previously [34] demonstrated that α-SiO_2, α-Al_2O_3, and $3Al_2O_3 \cdot 2SiO_2$ were the predominant crystalline phases; trace amounts of a cordierite phase were also detected.

Haydite as granules 2–3 mm in diameter (OOO SKhP Elita-Flora, Tomsk, Russia) and glass foam as granules 3–4 mm in diameter (ZAO Penosital, Perm, Russia) were used as granulated supports.

Nickel hydroxide was supported by homogeneous precipitation. For this purpose, a starting support was placed in a glass vessel with a solution of nickel nitrate and urea in a molar ratio of 1 : 10 and this vessel was heated in a water bath at 85 ± 1°C. In the course of synthesis, the following parameters were varied: nickel nitrate concentration (0.01–0.08 mol/l); precipitation time (1–5 h); and support/solution ratio, which is equal to the ratio of the support weight to the solution volume (0.08–0.44 g/ml). The support with supported nickel hydroxide was washed with distilled water and dried under an IR lamp for 4–6 h. The amount of nickel (wt %) precipitated on the surface was determined by atomic absorption spectrometry using an ASSIN instrument with a flame-ionization detector. The fraction of nickel precipitated on the surface (η, %) was calculated as follows:

$$\eta = \frac{\text{amount of precipitated nickel, g}}{\text{total amount of nickel in the starting solution, g}} \times 100.$$

The synthesis of CFC on the surface of aluminosilicate supports was performed by the pyrolysis of a propane–butane gas mixture. The support with supported nickel hydroxide was placed onto a glass filter (d = 25 mm; l = 200 mm) sealed in a tubular quartz reactor, which was placed in a vertical furnace with a fan. The temperature of the furnace was controlled using a PROTERM-100 microprocessor temperature regulator.

Gases were fed at the bottom through a glass filter. Initially, the sample was additionally dried in a flow of nitrogen (14 l/h) at 85°C for 30 min; then, the flow of nitrogen was changed to a flow of hydrogen (3 l/h), the temperature was increased to 500°C at a rate of 10 K/min, and the reduction of nickel hydroxides with hydrogen was performed for 30 min. Next, pyrolysis was performed at 500°C for 30 min by replacing the flow of hydrogen with a flow of a propane–butane mixture (6.4 l/h). The flow rates of gases were adjusted with a fine-adjustment regulator in a gas supply unit and measured with a soap bubble flow meter. The conversion of the propane–butane mixture fed into the reactor was no higher than 15%. In particular experiments, the process temperature was decreased to 400–450°C and the CFC synthesis time was increased to 8 h. The amount of carbon synthesized on the surface was determined gravimetrically from either the increase in the support weight, which was measured before and after pyrolysis, or the weight loss upon annealing the support in an atmosphere of oxygen at 800°C for 3 h.

The supports prepared in this study were characterized by the following physicochemical techniques: The specific surface areas of supports (S_{BET}, m^2/g) were determined using the thermal desorption of argon. The pore-size distribution was determined by mercury porosimetry on a Micromeritics AUTO-PORE 9200 instrument.

The crushing strength of supports under static conditions was measured on an MP-2S strength meter (Experimental Plant of the Siberian Branch of the Russian Academy of Sciences, Novosibirsk, Russia). The measurements were performed in both parent M/900 honeycomb monoliths with a circular cross section and the monoliths with a deposited carbon layer. The load (kg) at which a honeycomb monolith was crushed was normalized to the external geometric surface area (cm^2), which is equal to the product of the circumference of the cross section of the honeycomb monolith and the length of this monolith.

The electron-microscopic studies of the morphologies of supported nickel hydroxide and a synthesized CFC layer were performed with the use of JSM 6460 LV and LEO 1430 scanning electron microscopes.

RESULTS AND DISCUSSION

Supporting of Nickel Hydroxide on the Surface of Aluminosilicate Supports

It is well known [28, 31, 35] that the precipitation of hydroxides is a zero-order reaction with respect to the precipitated cation; this process is independent of the nature of the cation and depends completely on the rate of urea hydrolysis (I). With consideration for the rate constant of urea decomposition at 85°C (1.0×10^{-5} s^{-1} [31]), we calculated the conversion of urea depending on reaction time for a 0.1 M urea solution and related the resulting amount of hydroxide ions to the initial concentration of nickel ions in the reaction medium. Table 1 summarizes the results of these calculations. It can be seen that, at a 1 : 10 molar ratio of nickel nitrate to urea, it is sufficient for the complete conversion of nickel nitrate into the hydroxide to perform the process of homogeneous precipitation for 3 h. The resulting experimental data are consistent with these calculated data, and they demonstrate that Ni^{2+} can be completely precipitated from solution ($\eta = 100\%$) onto the surface of honeycomb monoliths for 3 h at a reaction temperature of 85°C and a 1 : 10 molar ratio of nickel nitrate to urea under specially chosen conditions (Table 2).

Table 1. Calculated data for the decomposition of a 0.1 M urea solution at 85°C depending on reaction time

Reaction time, h	Urea conversion, %	Ni^{2+}/OH^-*, mol/mol
1	4	1 : 0.8
3	10	1 : 2.0
5	17	1 : 3.4

* Obtained by relating the amount of liberated hydroxide ions to the amount of nickel ions in the starting solution at a 1 : 10 molar ratio between nickel nitrate and urea.

According to Ketov [28], the colloidal particles of nickel hydroxide formed in the course of homogeneous precipitation can aggregate with other particles in the bulk of solution and undergo sedimentation (deposition) onto the surface of a support. A decrease in the concentration of nickel in solution and/or an increase in the ratio of the amount of the support to the solution volume decreases the probability of particle aggregation in solution and increases the probability of deposition of the colloid particle of nickel hydroxide onto the support surface. In this case, it is of importance to take into account the support amount loaded in the solution, based on the geometric surface area of the support. The results obtained in this work for aluminosilicate honeycomb monoliths prepared based on clay, talc, and amorphous aluminum hydroxide are consistent with published data [28] on the effects of time, initial solution concentrations, and the ratio of the support amount loaded to the solution volume on the distribution of nickel in the system.

Thus, we found that the fraction of precipitated nickel (η) increased to 100% in M/900 honeycomb monoliths as the support/solution ratio was increased from 0.08 to 0.16 g/ml. Analogous results were obtained in the M/1300 support (Table 2). The amount of supported nickel can increase at a low support/solution ratio because of an increase in the duration of homogeneous precipitation (Fig. 1). It can be seen that the amount of nickel precipitated onto a support linearly increased as the synthesis time was increased from 1 to 5 h. The concentration of nickel on the support surface also increased with an increase in the concentration of nickel nitrate (by a factor of 2–4) and, cor-

Table 2. Effect of the ratio of the support amount to the solution volume on the nickel concentration on the surface of honeycomb aluminosilicate monoliths

Support	Initial concentration of $Ni(NO_3)_2$, mol/l	Support/solution ratio, g/ml	Concentration of supported Ni, wt %	η, %	S_{BET}, m^2/g	
					parent support	support with Ni
M/900	0.01	0.08	0.49	65	24	26
M/900	0.01	0.16	0.38	100	24	–
M/1030	0.02	0.08	0.58	41	10	12
M/1030	0.02	0.44	0.31	100	10	13

Note: Molar ratio $[Ni(NO_3)_2]/[(NH_2)_2CO] = 1 : 10$; synthesis time, 3 h; $T = 85°C$.

respondingly, urea (Fig. 2). However, in this case, η decreased to 69%; this was likely due to an increase in the fraction of aggregated hydroxide particles in solution and sedimentation at the bottom of the flask.

Along with factors such as reaction time, initial solution concentrations, and specific surface areas of supports, the temperature of monolith calcination considerably affected the fraction of nickel precipitated on the surface of a honeycomb monolith (Table 3). We found that the fraction of precipitated nickel and the weight concentration of nickel in supports decreased as the calcination temperature of the honeycomb monolith was increased. It is likely that the adsorption capacity of the surface of honeycomb monoliths toward colloidal nickel hydroxide particles decreased in the course of agglomeration, which was accompanied by a phase transition and a dramatic decrease (by orders of magnitude) in the specific surface area (Table 3). Low concentrations of supported nickel were also characteristic of other supports calcined at high temperatures with undeveloped specific surface areas—ceramic foam, haydite, and glass foam (Table 4).

The electron-microscopic study of samples revealed the homogeneity of the nickel coatings synthesized on the aluminosilicate supports. The electron micrograph of the surface of the M/900 aluminosilicate honeycomb monolith with supported nickel hydroxide indicates that the surface of this support was uniformly and densely coated with flake nickel hydroxide particles (Fig. 3). As the calcination temperature was increased, a cordierite phase was formed and the specific surface area of the support dramatically decreased (Table 3); this resulted in a considerable decrease in the amount of supported nickel and in an increase in the particle size of nickel hydroxide on the support surface (Fig. 4a). In this case, the texture of the support surface had a considerable effect on the fixation and localization of nickel hydroxide particles on the support. Deposited particles were mainly arranged on a poorly crystallized cordierite surface at the edges of faces, and they were practically absent from well-crystallized faces

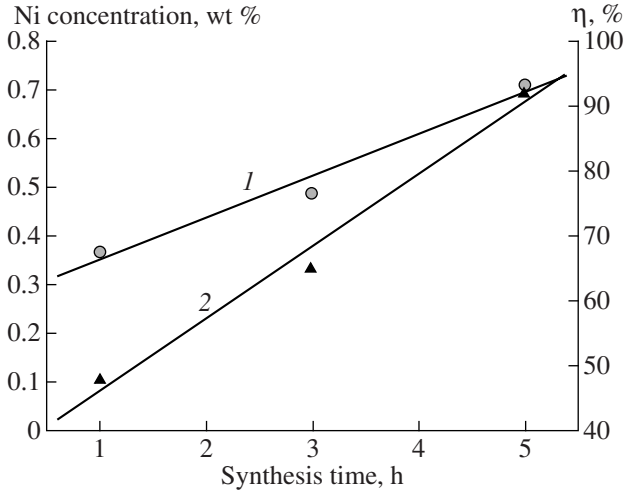

Fig. 1. Effect of synthesis time on (*1*) the amount of nickel supported on M/900 and (*2*) the fraction of precipitated nickel (η). $[Ni(NO_3)_2] = 0.01$ mol/l; $[(NH_2)_2CO] = 0.1$ mol/l; support/solution = 0.08 g/ml; $T = 85°C$.

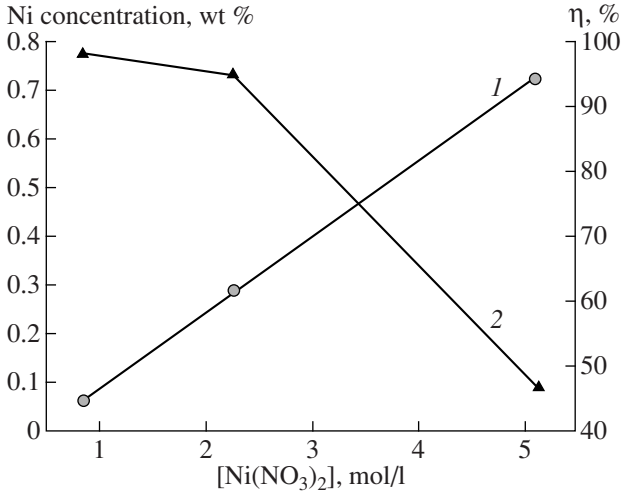

Fig. 2. Effect of the initial concentration of nickel nitrate on (*1*) the amount of nickel supported on M/1030 and (*2*) the fraction of precipitated nickel (η). Molar ratio $[Ni(NO_3)_2]/[(NH_2)_2CO] = 1 : 10$; support/solution = 0.34–0.44 g/ml; synthesis time, 3 h; $T = 85°C$.

Table 3. Effect of the calcination temperature of the parent honeycomb aluminosilicate monolith on the amount of supported nickel

Support	Supported Ni content, wt %	η, %	S_{BET}, m^2/g	
			parent support	support with Ni
M/900	0.38	100	24.0	23.4
M/1100	0.14	37	0.9	1.2
M/1200	0.04	17	~0.1	~0.1

Note: $[Ni(NO_3)_2]$ = 0.01 mol/l; $[(NH_2)_2CO]$ = 0.1 mol/l; support/solution ratio, 0.15–0.16 g/ml; synthesis time, 3 h; T = 85°C.

Table 4. Supporting of nickel by homogeneous precipitation in the presence of urea onto aluminosilicate foam materials

Support	Support/solution ratio, g/ml	Supported Ni content, wt %	η, %	S_{BET}, m^2/g	
				parent support	support with Ni
Ceramic foam	0.16	0.12	34	0.2	0.3
Glass foam	0.03	0.26	16	0.4	1.2
Haydite	0.16	0.07	19	1.0	1.3

Note: $[Ni(NO_3)_2]$ = 0.01 mol/l; $[(NH_2)_2CO]$ = 0.1 mol/l; synthesis time, 3 h; T = 85°C.

(Fig. 4a). It is likely that the denser coverage of the surface of M/900 with nickel hydroxide particles, as compared with that of M/1200, was due to the more imperfect structure of its surface. The appearance of irregular coarse aggregated particles (≥0.5 μm) was a special feature of the morphology of the nickel coating on the surface of M/1200 (Fig. 4b).

The potential of homogeneous precipitation is so great that it allows one to support a nickel coating onto a glass surface. The electron micrograph of a glass foam surface with supported nickel hydroxide indicates that the smooth nonporous glass surface was almost completely covered with small particles (Fig. 5). In this case, both regions with dense clusters of ordered particles and open surface regions are observed.

As in the case of M/1200, spherical aggregates of coarser flat particles of nickel hydroxide were present on the surface of glass foam. The formation of aggregates from the flat particles of nickel hydroxide in the homogeneous precipitation of nickel with urea in the absence of supports was also described previously [36, 37]. We assume that the presence of a small amount of coarse particles on the surface of a support is characteristic of samples, the synthesis of which was characterized by a low value of η (the fraction of nickel hydroxide precipitated on the surface) and it is due to the random immobilization of aggregates formed in solution.

Synthesis of a CFC Layer on the Surfaces of Supports

We studied the catalytic pyrolysis of a propane–butane mixture and found that the amount of synthesized carbon increased with the reaction temperature (Fig. 6). A change in the CFC synthesis time from 0.5 to 8.0 h resulted in an insignificant increase of carbon (by ~10%). Table 5 summarizes the main characteristics of supports with a synthesized CFC layer prepared at a process temperature of 500°C and a time of 0.5 h.

In the course of pyrolysis, all of the samples acquired a uniform rich velvety black shade. Upon cleaving a honeycomb monolith, we found that the formation of carbon occurred on the outer side of the wall; CFC was almost not formed within the pore space of the support walls (Figs. 7, 8c, 9b). It is likely that this special feature of the synthesis of the carbon coating was related to the stage of supporting nickel hydroxide in the course of homogeneous precipitation in the presence of urea, which allowed us to form sufficiently

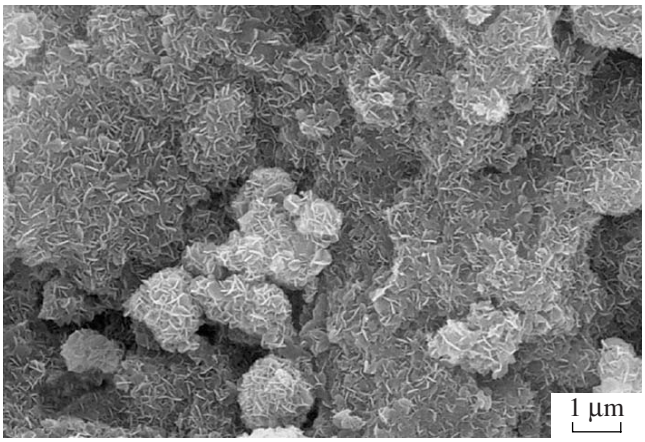

Fig. 3. Electron micrograph of the surface of the M/900 honeycomb monolith with supported nickel hydroxide. The nickel content of the support is 0.71 wt %.

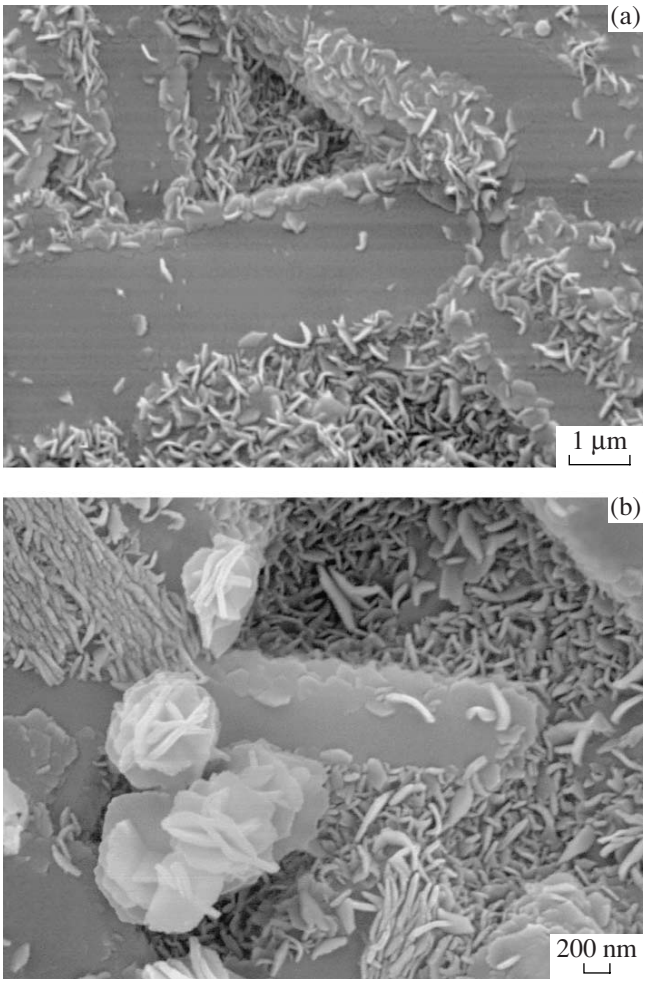

Fig. 4. Electron micrographs of the surface of the M/1200 honeycomb monolith with supported nickel hydroxide. The nickel content of the support is 0.04 wt %.

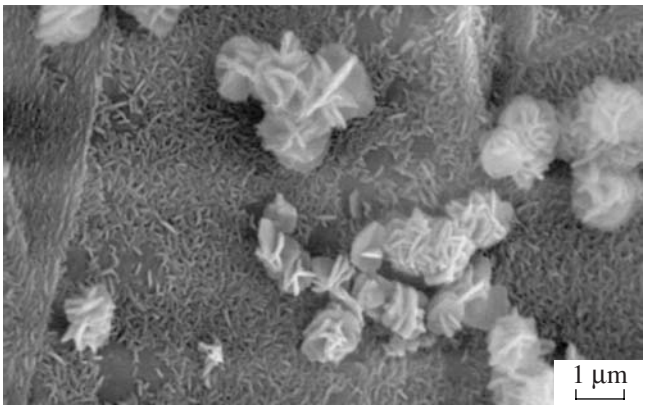

Fig. 5. Electron micrograph of the surface of glass foam with supported nickel hydroxide. The nickel content of the support is 0.26 wt %.

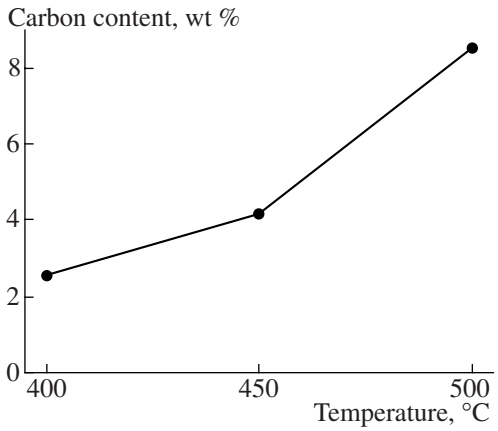

Fig. 6. Effect of the pyrolysis temperature of a propane–butane mixture on the amount of carbon supported on the surface of M/900.

large nickel hydroxide particles on the outer geometric surface of ceramic supports. Moreover, the use of low-concentration solutions of nickel nitrate facilitated a decrease in the concentration of Ni^{2+} in pores on impregnating the support at the instant the support was immersed in the initial solution. A CFC layer was not formed within the pore space of support walls in the course of pyrolysis, and the mechanical strength of parent macrostructured supports changed insignificantly after the synthesis of the carbon layer (Table 6). With

Table 5. Main characteristics of honeycomb aluminosilicate monoliths with a synthesized CFC layer

Support	Supported Ni content, wt %	Carbon content, wt %	S_{BET}, m^2/g	
			parent support	support with a CFC layer
M/900	0.37	4.8	24.0	47.0
	0.71	10.4		69.0
M/1030	0.31	0.2	10.0	15.0
	0.52	1.0		22.0
	0.93	4.9		48.0
M/1100	0.14	3.4	0.9	16.0
M/1200	0.04	0.5	0.1	0.8

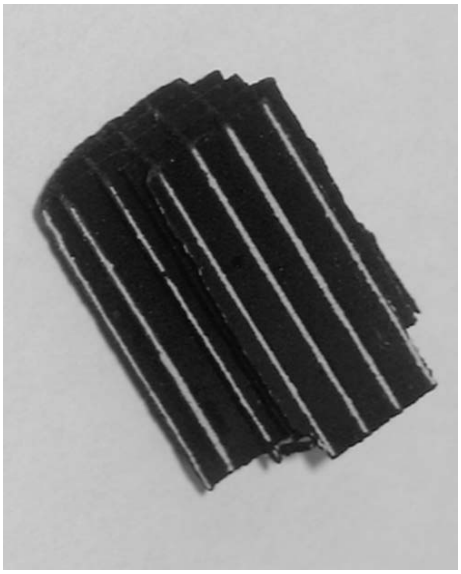

Fig. 7. Image of a cleavage of the M/900 honeycomb monolith with a supported carbon layer.

the use of the impregnation method for introducing nickel compounds into the M/900 honeycomb monolith, a decrease in its mechanical strength was observed even at a sufficiently low carbon content.

Using scanning electron microscopy, we found that the distribution of formed nickel metal particles over the surface of the M/1200 support remained unchanged at the step of nickel hydroxide reduction with hydrogen. Nickel metal particles, as well as nickel hydroxide particles (Fig. 4), were localized on the more imperfect surface of the support, and they were absent from well-crystallized faces (Fig. 8a). In the course of pyrolysis, a loose carbon layer was synthesized on the surface of M/1200; this layer consisted of relatively long and thick carbon fibers (Fig. 8b). The thickness of the synthesized carbon fibers was consistent with the particle size of nickel metal.

The carbon layer synthesized on the M/900 support (nickel hydroxide was deposited as relatively small particles on the comparatively rough surface of this support (Fig. 3)) was formed by relatively short carbon fibers interwoven with each other (Fig. 9a). It is likely

Table 6. Crushing strength of M/900 supports under static conditions

Carbon content, wt %	Strength, kg/cm^2	Average strength, kg/cm^2
0	6.6	5.1
	4.3	
	4.4	
5.5	5.1	4.6
6.6	4.6	
7.2	4.2	

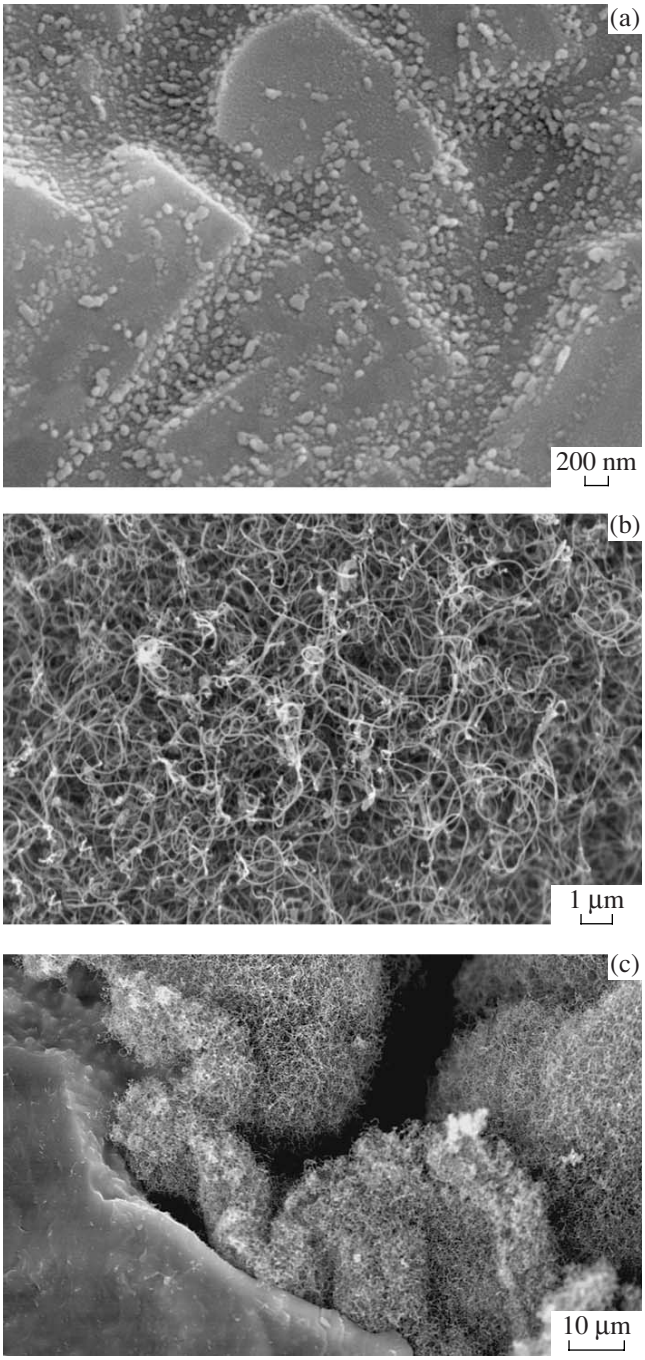

Fig. 8. Electron micrographs of the surface of the M/1200 cordierite honeycomb monolith with (a) Ni^0 particles and (b, c) a synthesized CFC layer. The carbon content was 0.5 wt %. The mark corresponds to a distance of (a) 200 nm, (b) 1 μm, or (c) 10 μm.

that, in this case, smaller nickel metal particles were formed in the course of reduction because it is well known that the particle size of Ni^0 is responsible for the length and thickness of the synthesized carbon fiber, as well as for the initial rate of carbon formation, the rate of catalyst deactivation, and the final yield of carbon in the catalytic pyrolysis of hydrocarbons [17, 20, 21, 24].

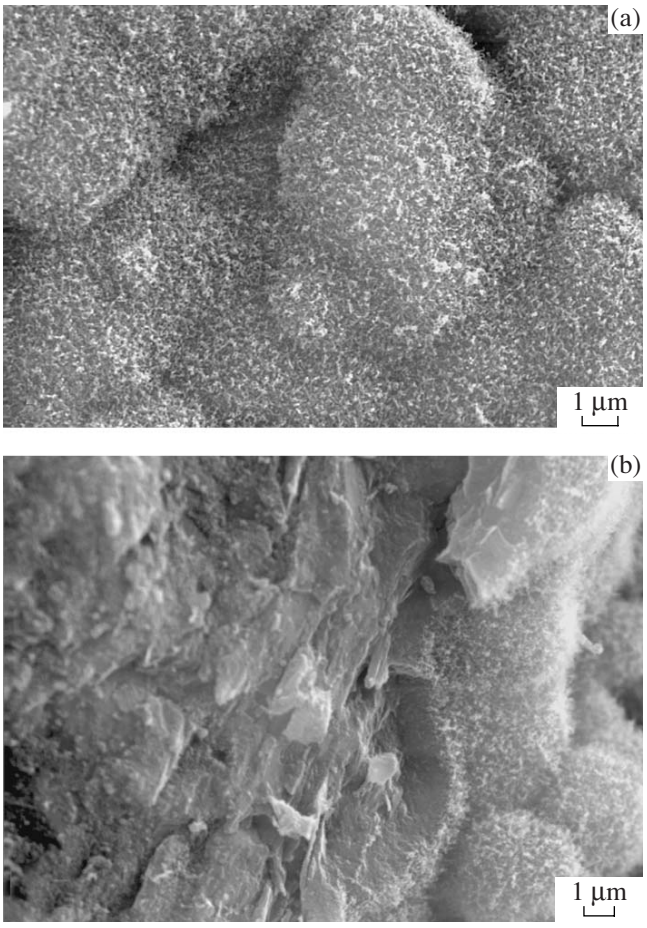

Fig. 9. Electron micrographs of the surface of the M/900 honeycomb monolith with a synthesized CFC layer (a) and a cleavage (b). The carbon content was 10.4 wt %.

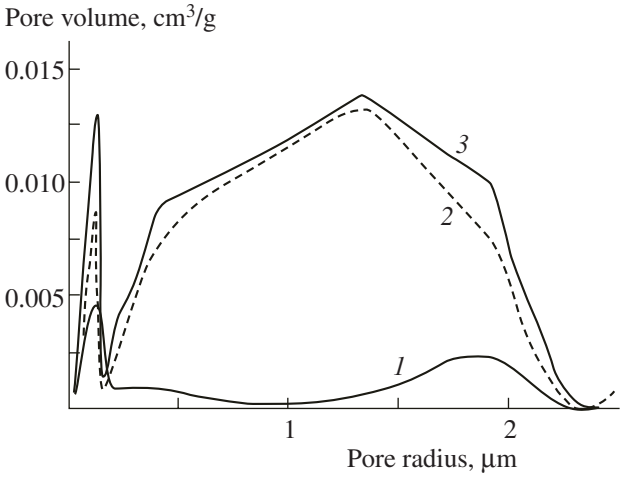

Fig. 10. Pore-size distribution diagrams of (*1*) the M/1200 honeycomb monolith and (*3*) the CFC-containing support and (*2*) the calculated pore-size distribution diagram for a carbon layer.

An analysis of data given in Table 5 indicates that the concentration of CFC supported onto the honeycomb monoliths increased with the nickel content. In this case, the synthesis of a porous CFC layer was accompanied by a considerable increase in the specific surface area of the support. We separately estimated the specific surface area of the carbon layer taking into account the increase of the specific surface area of the support, as compared with that of the starting matrix, and the increase of the weight of carbon in the course of pyrolysis. We found that the carbon layer synthesized on the M/900, M/1030, and M/1100 supports was characterized by a specific surface area higher than 300 m^2/g. For the carbon layer synthesized on the M/1200 support, the specific surface area was 100–150 m^2/g.

For the M/1200 support with a pore volume smaller than 0.1 cm^3/g and a specific surface area of 0.1 m^2/g, the pore-size distribution diagrams of the starting matrix (Fig. 10, curve *1*) and the carbon-containing support (Fig. 10, curve *3*) were dramatically different. Comparing these pore-size distribution diagrams, we can separately obtain a pore-size distribution for the carbon layer (Fig. 10, curve *2*). It can be seen that the carbon layer on M/1200 was characterized by the presence of pores of size to 1 μm or higher; this is consistent with electron-microscopic data (Fig. 8). For the M/900 aluminosilicate support with a pore volume of 0.25 cm^3/g and a specific surface area of 24.0 m^2/g, we failed to determine correctly the contribution of the carbon coating to the pore structure of the CFC-containing support because the pore volume of the carbon layer constituted an insignificant fraction of the total pore volume of the carbon-containing M/900 aluminosilicate support.

CONCLUSIONS

Thus, we experimentally demonstrated that the homogeneous precipitation of nickel in the presence of urea is effective for supporting nickel hydroxide particles onto the surface of high-temperature macrostructured aluminosilicate supports: honeycomb monoliths, cellular ceramic foam, glass foam, and haydite. We found that the concentration of nickel on the surface of a support depends on the process conditions of homogeneous precipitation (time, starting solution concentrations, and loaded support amount). From the electron-microscopic data, it follows that the texture of an aluminosilicate surface plays an important role in the localization of nickel particles. The reduction of supported nickel hydroxide in hydrogen and the catalytic pyrolysis of a propane–butane mixture on a nickel metal catalyst allowed us to synthesize high-porosity carbon layers on the surface of supports with the retention of the mechanical strength and macrostructure of the parent aluminosilicate matrix.

ACKNOWLEDGMENTS

We are grateful to A.A. Ketov and V.B. Fenelonov for their fruitful collaboration and discussions of the results.

REFERENCES

1. Serp, P., Corrias, M., and Kalck, P., *Appl. Catal., A*, 2003, vol. 253, p. 337.
2. Salman, F., Park, C., and Baker, R.T., *Catal. Today*, 1999, vol. 53, p. 385.
3. Changhai Liang, Zhonglai Li, Jieshan Qiu, and Can Li, *J. Catal.*, 2002, vol. 211, p. 278.
4. Ros, T.G., Keller, D.E., van Dillen, A.J., et al., *J. Catal.*, 2002, vol. 211, p. 85.
5. Park, C. and Keane, M.A., *J. Colloid Interface Sci.*, 2003, vol. 266, p. 183.
6. Fenelonov, V.B., Derevyankin, A.Yu., Okkel, L.G., et al., *Carbon*, 1997, vol. 35, p. 1129.
7. Timofeeva, M.N., Matrosova, M.M., Reshetenko, T.V., et al., *J. Mol. Catal., A: Chem.*, 2004, vol. 211, p. 131.
8. Reshetenko, T.V., Avdeeva, L.B., Ismagilov, Z.R., and Chuvilin, A.L., *Carbon*, 2004, vol. 42, p. 143.
9. Hitoshi Ogihara, Sakae Takenaka, Ichiro Yamanaka, and Kiyoshi Otsuka, *Carbon*, 2004, vol. 42, p. 1609.
10. Kiyoshi Otsuka, Hitoshi Ogihara, and Sakae Takenaka, *Carbon*, 2003, vol. 41, p. 223.
11. Kovalenko, GA., Kuznetsova, E.V., Mogilnykh, Yu.I., et al., *Carbon*, 2001, vol. 39, p. 1033.
12. Keller, N., Rebmann, G., Barraud, E., et al., *Catal. Today*, 2005, vol. 101, p. 323.
13. Ismagilov, Z.R., Shikina, N.V., Kruchinin, V.N., et al., *Catal. Today*, 2005, vols. 102–103, p. 85.
14. Tribolet, P. and Kiwi-Minsker, L., *Catal. Today*, 2005, vols. 102–103, p. 15.
15. Randall, LV.W. and Lee, J., *Carbon*, 2003, vol. 41, p. 659.
16. Jarrah, N., van Ommen, J.G., and Lefferts, L., *Catal. Today*, 2003, vols. 79–80, p. 29.
17. Jarrah, N.A., van Ommen, J.G., and Lefferts, L., *J. Mater. Chem.*, 2004, vol. 14, p. 1590.
18. Haberecht, J., Krumeich, F., Stalder, M., and Nesper, R., *Catal. Today*, 2005, vols. 102–103, p. 40.
19. Sang-Dae Bae, Masaki Sagehashi, and Akiyoshi Sakoda, *Carbon*, 2003, vol. 41, p. 2973.
20. Wang, P., Tanabe, E., Ito, K., et al., *Appl. Catal., A*, 2002, vol. 231, p. 35.
21. De Chen, Kjersti, O.C., Ester, O.-F., et al., *J. Catal.*, 2005, vol. 229, p. 82.
22. Park, C. and Keane, M.A., *J. Catal.*, 2004, vol. 221, p. 386.
23. Vander Wal, R.L., Ticich, T.M., and Curtis, V.E., *Carbon*, 2001, vol. 39, p. 2277.
24. Katsuomi Takehira, Takenori Ohi, and Tetsuya Shishido, et al., *Appl. Catal., A*, 2005, vol. 283, p. 137.
25. Hongbin Zhao, Draelants, D.J., and Baron, G.V., *Catal. Today*, 2000, vol. 56, p. 229.
26. Vergunst, T., Kapteijn, F., and Moulijn, J.A., *Appl. Catal., A*, 2001, vol. 213, p. 179.
27. Xu Xiaoding, Vonk, H., van de Riet, A.C.J.M., Cybulski, A., et al., *Catal. Today*, 1996, vol. 30, p. 91.
28. Ketov, A.A., *Doctoral (Chem.) Dissertation*, Perm: Perm. State Tech. Univ., 1998.
29. Akinc, M., Jongen, N., Lemaitre, J., and Hofmann, H., *J. Eur. Ceram. Soc.*, 1998, vol. 18, p. 1559.
30. Zhao, Y.L., Wang, J.M., Chen, H., et al., *Int. J. Hydrogen Energy*, 2004, vol. 29, p. 889.
31. Seungman Sohn, Youngshik Kwon, Yeunsik Kim, and Dongsu Kim, *Powder Technol.*, 2004, vol. 142, p. 136.
32. Lathouder, K.M., Flo, T.M., Kapteijn, F., and Moulijn, J.A., *Catal. Today*, 2005, vol. 105, p. 443.
33. Khabas, T.A., Vereshchagin, V.I., Vakalova, T.V., et al., *Novye Ogneupory*, 2002, no. 4, p. 44.
34. Kovalenko, GA., Komova, O.V., Simakov, A.V., et al., *J. Mol. Catal., A: Chem*, 2002, vols. 182–183, p. 73.
35. Fazleev, M.P., Ketov, A.A., Ismagilov, Z.R., and Barannik, G.B., *Collected Works*, Ismagilov, Z.R., Ed., Novosibirsk: Inst. Kataliza, 1990, p. 10.
36. Durand-Keklikian, L., Haq, I., and Matijevi, E., *Colloids Surf., A*, 1994, vol. 92, p. 267.
37. Porta, F., Recchia, S., Bianchi, C., et al., *Colloids Surf., A*, 1999, vol. 155, p. 395.